15th Australasian Fluid Mechanics Conference
The University of Sydney, Sydney, Australia
13-17 December 2004

Flow of a Nonlinear Viscoelastic Fluid in Concentric Rotating Cylinders with relative rotation

M. Mirzazadeh[1] and F.Rashidi[1*] and S.H.Hashemabadi[2]

[1]Department of Chemical Engineering,
Amir kabir University of Technology, 424 Hafez Ave, Tehran, IRAN

[2]Department of Chemical Engineering,
Iran University of Science and Technology, 16844 Narmak, Tehran, IRAN

Abstract

An analytical solution is presented for the steady and purely tangential flow of a viscoelastic fluid obeying the simplified form of Phan-Thien-Tanner (PTT) constitutive equation in a concentric annulus with relative cylinder rotation. The effect of fluid elasticity and aspect ratio on the velocity profile and $f\mathrm{Re}$ are investigated for two combinations of inner and outer cylinder rotation. The results show that the differences between the radial location of the minimum velocity and of the critical angular velocity compared with their Newtonian counterparts increase when the fluid elasticity increases. The results also show that $f\mathrm{Re}$ decreases with increasing fluid elasticity and radius ratio in the case of inner cylinder rotation.

Introduction

An extensive bibliography of work on the flow of non-Newtonian liquids through annular channels is given in the recent paper by Escudier et al [1]. The flow of non-Newtonian fluids was studied in several works [2-6]. Cruz and Pinho [7] derived an analytical solution for helical flow within a concentric annulus of a fluid obeying the simplified form of the Phan-Thien-Tanner (SPTT) constitutive equation.

The PTT model is a non-linear viscoelastic constitutive equation derived using network theory by Phan-Thien and Tanner [8]. A distinctive advantage of the PTT model over most of the other similar constitutive equations is the inclusion of an elongational parameter ε. The flow of PTT viscoelastic fluids has been considered in several works by Oliveira and Pinho [9], Alves et al [10] and Hashemabadi et al [11].

The objective of the present investigation is to obtain velocity profiles as well as the coefficient of friction using an analytical method to solve the simplified form of PTT model in purely tangential flow between concentric rotating cylinders where the inner and outer cylinders are rotating with different angular velocities, for a wide range of fluid elasticity and radius ratios.

Mathematical Formulation

We assume steady-state, laminar, purely tangential flow and neglect body forces in the momentum equation. We then have:

$$V_\theta = V_\theta(r) \quad , \quad V_z = V_r = 0 \tag{1}$$

Where V_r , V_θ and V_z are the radial, tangential and axial components of velocity profile, respectively.

The dimensionless form of the momentum equation for the θ-direction is:

$$\frac{1}{\overset{*}{r}^2}\frac{d}{d\overset{*}{r}}(\overset{*}{r}^2\,\overset{*}{\tau}_{r\theta}) = 0 \tag{2}$$

The simplified form of the PTT constitutive equation is as follows:

$$Z(tr\,\tau)\tau + \lambda\tau_{(1)} = \eta\dot{\gamma} \tag{3}$$

Where η is the viscosity coefficient of the model, λ is the relaxation time, $tr\,\tau$ is the trace of stress tensor and $\tau_{(1)}$ is the convected time derivative of stress tensor:

$$\tau_{(1)} = \frac{D\tau}{Dt} - \{(\nabla V)^T.\tau + \tau.(\nabla V)\} \tag{4}$$

The stress coefficient, Z , has an exponential form:

$$Z(tr\,\tau) = \exp(\frac{\varepsilon\lambda}{\eta}tr\,\tau) \tag{5}$$

Where ε is the elongational parameter of the model. Eq. (5) may be linearized when the deformation rate of a fluid element is small which corresponds to the behaviour of weak flow according to Tanner's classification [12]:

$$Z(tr\,\tau) = 1 + \frac{\varepsilon\lambda}{\eta}tr\,\tau \tag{6}$$

Exact solution for the simplified PTT model (SPTT)

For steady tangential annular flow Eq. (3) reduces to:

$$Z(tr\,\tau)\tau_{\theta\theta} = 2\lambda\dot{\gamma}\tau_{r\theta} \tag{7}$$

$$Z(tr\,\tau)\tau_{rr} = 0 \tag{8}$$

$$Z(tr\,\tau)\tau_{r\theta} = \eta\dot{\gamma} + \lambda\dot{\gamma}\tau_{rr} \tag{9}$$

Eq. (8) indicates $\tau_{rr} = 0$, hence the trace of the stress tensor will be equal to $\tau_{\theta\theta}$. Using Eq. (6) for the stress coefficient yields:

$$Z = 1 + \frac{\varepsilon\lambda}{\eta}\tau_{\theta\theta} \tag{10}$$

By dividing Eq. (9) by Eq. (7) the following for $\tau_{\theta\theta}$ is obtained:

$$\tau_{\theta\theta} = \frac{2\lambda}{\eta}\tau_{r\theta}^2 \tag{11}$$

The shear rate $\dot{\gamma}$ is obtained by substituting $\tau_{\theta\theta}$ from Eq. (11) into Eq. (7) and using Eq. (10) for the stress coefficient:

$$\eta\dot{\gamma} = \tau_{r\theta}\left[1 + \frac{2\varepsilon\lambda^2}{\eta^2}\tau_{r\theta}^2\right] \tag{12}$$

where the shear rate $\dot{\gamma}$ is defined by:

$$\dot{\gamma} = r\,\frac{d}{dr}\left(\frac{V_\theta}{r}\right) \tag{13}$$

The dimensionless shear stress is obtained by integrating Eq. (2):

$$\frac{\overset{*}{\tau}_{r\theta}}{\overset{*}{\tau}_{wi}} = \frac{\kappa^2}{\overset{*}{r}^2} \tag{14}$$

Where $\overset{*}{\tau}_{wi}$ is the dimensionless wall shear stress on the inner cylinder and κ is inner to outer radius ratio (R_i / R_o).

Combination of Eqs. (12) and (13) leads to:

$$(1-\kappa)\overset{*}{r}\ \frac{d}{d\overset{*}{r}}\left(\frac{\overset{*}{V_\theta}}{\overset{*}{r}}\right)=\left(1+2\varepsilon We^2\ \overset{*}{\tau}{}_{r\theta}^{2}\right)\overset{*}{\tau}_{r\theta} \qquad (15)$$

The following normalizations have been used in Eq. (15):

$$\overset{*}{r}=\frac{r}{R_o},\ \overset{*}{V_\theta}=\frac{V_\theta}{V_c},\ \overset{*}{\tau}_{r\theta}=\frac{\tau_{r\theta}}{\eta V_c/\delta},\ We=\lambda\frac{V_c}{\delta} \qquad (16)$$

Where We is the Weissenberg number, δ is the annular gap ($\delta = R_o - R_i$) and V_c is a characteristic velocity which is defined as follows:

$$V_c = \begin{cases} R_i\Omega_i & \Omega_o = 0 \\ R_o\Omega_o & \Omega_i = 0 \\ \bar{R}\left|\Omega_o - \Omega_i\right| & \Omega_i \neq \Omega_o \neq 0 \end{cases} \qquad (17)$$

Where $\bar{R}$ is the average radius ($(R_o + R_i)/2$). By substitution of $\overset{*}{\tau}_{r\theta}$ from Eq. (14) into Eq. (15) and then integration of this equation, the dimensionless velocity profile is obtained, as follows:

$$\frac{\overset{*}{V_\theta}}{\overset{*}{r}}=-\frac{\kappa^2\overset{*}{\tau}_{wi}}{(1-\kappa)\overset{*}{r}{}^2}\left[\frac{1}{2}+\frac{\varepsilon We^2\kappa^4\overset{*}{\tau}{}_{wi}^{2}}{3\overset{*}{r}{}^4}\right]+C_2 \qquad (18)$$

The boundary conditions are as follows:

		Both	Inner	Outer	
$r=R_i$	$V_\theta=$	$R_i\Omega_i$	$R_i\Omega_i$	0	(19)
$r=R_o$	$V_\theta=$	$R_o\Omega_o$	$R_o\Omega_o$	0	(20)

and in dimensionless form:

$$\overset{*}{r}=\kappa \qquad \overset{*}{V_\theta}=\frac{2\kappa}{(1+\kappa)\left|\beta-1\right|} \qquad 1 \qquad 0 \qquad (21)$$

$$\overset{*}{r}=1 \qquad \overset{*}{V_\theta}=\frac{2\beta}{(1+\kappa)\left|\beta-1\right|} \qquad 0 \qquad 1 \qquad (22)$$

Where β is the outer to inner angular velocity ratio (Ω_o/Ω_i). By introducing boundary conditions from Eqs. (21) and (22) into Eq. (18), and after mathematical simplification, the following cubic equation is obtained:

$$\overset{*}{\tau}{}_{wi}^{3}+\mathrm{p}\,\overset{*}{\tau}_{wi}+\mathrm{q}=0 \qquad (23)$$

Where the constants p and q in Eq. (23) for the cases of both cylinder rotation, inner cylinder rotation and outer cylinder rotation are, respectively:

$$\mathrm{p}=\frac{3(1-\kappa^2)}{2\varepsilon We^2(1-\kappa^6)},\ \mathrm{q}=\frac{-6(1-\kappa)(\beta-1)}{\varepsilon We^2(1-\kappa^6)(1+\kappa)\left|\beta-1\right|} \qquad (24)$$

$$\mathrm{p}=\frac{3(1-\kappa^2)}{2\varepsilon We^2(1-\kappa^6)},\ \mathrm{q}=\frac{3(1-\kappa)}{\varepsilon We^2(1-\kappa^6)\ \kappa} \qquad (25)$$

$$\mathrm{p}=\frac{3(1-\kappa^2)}{2\varepsilon We^2(1-\kappa^6)},\ \mathrm{q}=\frac{-3(1-\kappa)}{\varepsilon We^2(1-\kappa^6)} \qquad (26)$$

The real solution of Eq. (23) can be expressed as:

$$\overset{*}{\tau}_{wi}=\frac{1}{6}\sqrt[3]{-108\,\mathrm{q}+12\sqrt{12\,\mathrm{p}^3+81\,\mathrm{q}^2}}-2\,\mathrm{p}/\sqrt[3]{-108\,\mathrm{q}+12\sqrt{12\,\mathrm{p}^3+81\,\mathrm{q}^2}} \qquad (27)$$

By introducing boundary conditions from Eq. (21) or (22) into Eq. (18) and using $\overset{*}{\tau}_{wi}$ from Eq. (27), the second constant C_2 can be easily obtained.

For the limiting case of a Newtonian fluid ($\varepsilon We^2 \to 0$), Eq. (18) reduces to:

$$\frac{\overset{*}{V_\theta}}{\overset{*}{r}}=-\frac{\kappa^2\overset{*}{\tau}_{wi}}{2(1-\kappa)}\frac{1}{\overset{*}{r}{}^2}+C_2 \qquad (28)$$

By introducing boundary conditions from Eqs. (21) and (22) into Eq. (28), the following relations can be written to obtain $\overset{*}{\tau}_{wi}$ and C_2 for the cases of both, inner and outer cylinder rotation, respectively :

$$\overset{*}{\tau}_{wi}=\frac{4(\beta-1)}{(1+\kappa)^2\left|\beta-1\right|} \qquad C_2=\frac{2(\beta-\kappa^2)}{(1+\kappa)(1-\kappa^2)\left|\beta-1\right|} \qquad (29)$$

$$\overset{*}{\tau}_{wi}=-\frac{2}{\kappa(1+\kappa)} \qquad C_2=-\frac{\kappa}{(1-\kappa^2)} \qquad (30)$$

$$\overset{*}{\tau}_{wi}=\frac{2}{(1+\kappa)} \qquad C_2=\frac{1}{1-\kappa^2} \qquad (31)$$

These results are in full agreement with previous work such as that of Mahmud and Fraser [13].

An important parameter in engineering calculations is the product of the friction factor and the Reynolds number. In the present situation, the torque friction factor, f, can be defined as follows [14]:

$$\mathrm{f}=\frac{\tau_w}{\rho V_c^2/2} \qquad (32)$$

and the rotational Reynolds number as [6,14]:

$$\mathrm{Re}=\rho V_c\,\delta/\eta \qquad (33)$$

Using these definitions we can derive the following equations for the two special cases of inner and outer cylinder rotation ($\mathrm{fRe_i}$ and $\mathrm{fRe_o}$):

$$\mathrm{fRe_i}=-2\,\overset{*}{\tau}_{wi} \qquad (34)$$

$$\mathrm{fRe_o}=2\kappa^2\,\overset{*}{\tau}_{wi} \qquad (35)$$

Results and Discussion

Velocity profiles are presented in figure 1, for different values of the angular velocity ratio (β). As represented in this figure, the velocity profile shows a minimum value within the annular gap for $\beta > \beta_c$. The radial location of the minimum velocity can be determined from the following equation:

$$\overset{*}{r}_{\min}=\frac{\sqrt{6d\,(d^2+4a^2-2ad)}}{6d} \qquad (36)$$

where

$$d=\sqrt[3]{(-108\,b-8a^3+12\sqrt{(81b^2+12ba^3)}} \qquad (37)$$

$$a=\frac{\kappa^2\overset{*}{\tau}_{wi}}{2(1-\kappa)C_2} \qquad (38)$$

$$b=\frac{5\varepsilon We^2\kappa^6\overset{*}{\tau}_{wi}}{3C_2} \qquad (39)$$

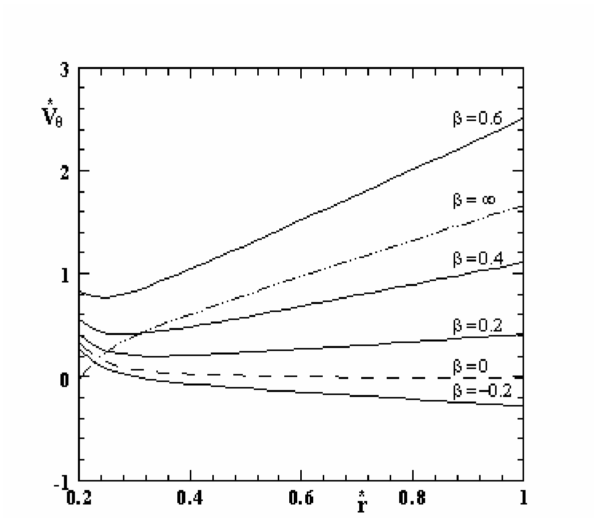

Figure 1. Effect of angular velocity ratio on velocity profile for $\kappa = 0.2$ and $\varepsilon We^2 = 10$.

For the limiting case of a Newtonian fluid (i.e. $\varepsilon We^2 \to 0$), we arrive at the well-known (see e.g. [13]) result:

$$\overset{*}{r}_{\min} = \kappa \sqrt{(1-\beta)/(\beta-\kappa^2)} \tag{40}$$

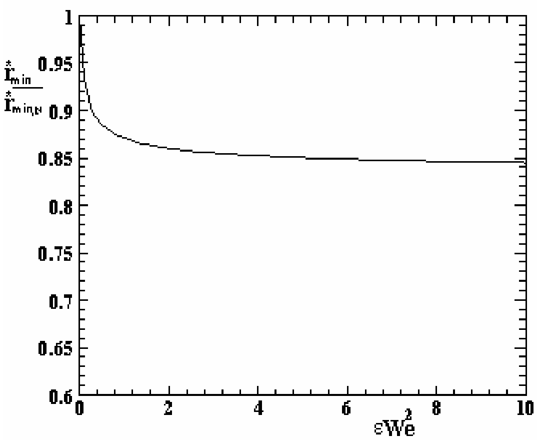

Figure 2. Effect of fluid elasticity, εWe^2 , on the radial location of minimum velocity for $\kappa = 0.5$.

Figure 2, shows the location of minimum velocity ($\overset{*}{r}_{\min}$), normalized with the corresponding Newtonian values (according to Eq. (40)) as a function of the non-dimensional viscoelastic group (εWe^2). As can be seen, the departure from the Newtonian value increases with increasing fluid elasticity.
As can be seen from figure 1, the velocity profile exhibits a minimum when β is greater than a critical value (β_c) which satisfies the following inequality:

$$\kappa < \overset{*}{r}_{\min} < 1 \tag{41}$$

Figure 3, shows the critical value of the angular velocity ratio, β_c , normalized with the corresponding Newtonian value ($\beta_{c,N} = 2\kappa^2 /(1+\kappa^2)$) as a function of the elasticity parameter (εWe^2), for the various values of the radius ratio κ .

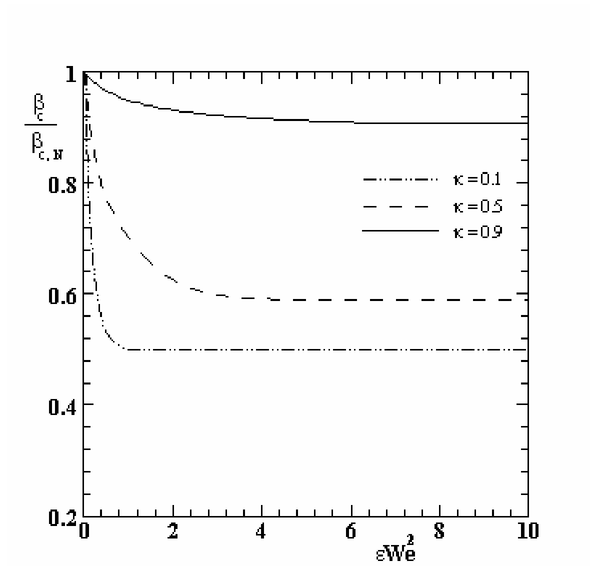

Figure 3. Effect of fluid elasticity, εWe^2 , and radius ratio (κ) on critical angular velocity.

For high values of κ , i.e. for a narrow annulus, β_c is only marginally different from the Newtonian value and is independent of elasticity for large value of εWe^2 . For smaller radius ratios, for example $\kappa = 0.1$, the differences are about 50% at high Weissenberg number.

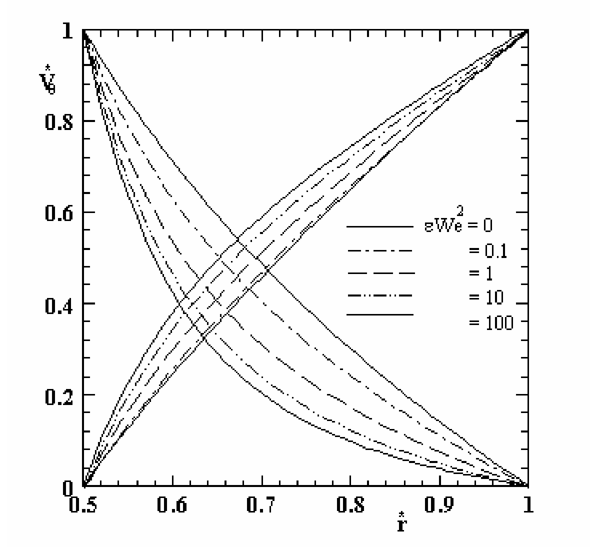

Figure 4. Effect of fluid elasticity, εWe^2 , on the velocity profile in the both cases of inner and outer cylinder rotation for $\kappa = 0.5$.

Figure 4, shows the effect of fluid elasticity on the velocity profile for the two special cases of inner and outer cylinders rotation. As can be seen, by increasing fluid elasticity εWe^2 the velocity profile differs from the Newtonian case, i.e. as the shear-thinning behaviour of the fluid increases. The viscosity function and shear-thinning behaviour of a PTT fluid is discussed in detail by Pinho and Oliveria [15] and Alvez, et al [10].
The influence of the radius ratio on the velocity profile for the two special cases of inner cylinder rotation and outer cylinder

rotation are shown in Figure 5. The results show that the profiles tend to take linear form with increasing κ .

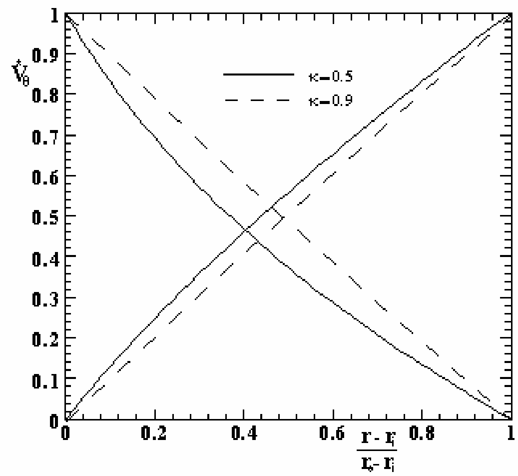

Figure 5 Effect of radius ratio on velocity profile in the both cases of inner and outer cylinder rotation for, $\varepsilon We^2 = 0.01$.

Figure 6, shows the effect of fluid elasticity on $f\mathrm{Re}$ which is normalized with the corresponding Newtonian value ($f\mathrm{Re}_{i,N} = 4/\kappa(1+\kappa)$) for the various radius ratios for the case of inner cylinder rotation

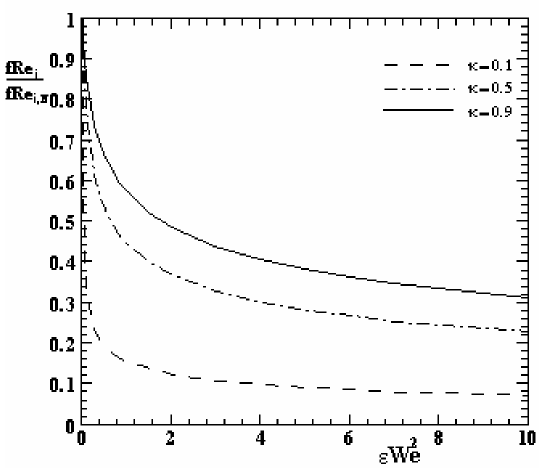

Figure 6. Effect of fluid elasticity, εWe^2 , and radius ratio (κ) on the ratio of viscoelastic to Newtonian friction factor ($f\mathrm{Re}_i / f\mathrm{Re}_{i,N}$) .

The decrease in $f\mathrm{Re}$ with increasing elasticity is again attributable to the shear-thinning behaviour of the PTT fluid. As can be seen from this figure, as εWe^2 approaches zero the $f\mathrm{Re}$ values are in agreement with those for a Newtonian fluid [6 and 14]. These features of polymeric fluid have been investigated experimentally by Escudier et al. [16]. Their results showed that increasing fluid elasticity decreases friction factor. The same conclusion will be achieved if we plot $f\mathrm{Re}_o$ against εWe^2 .

Conclusion

An analytical solution has been derived for the steady-state, purely tangential flow in a concentric annulus with relative rotation of the two cylinders of a viscoelastic fluid obeying the simplified form of the Phan-Thien-Tanner (PTT) constitutive equation. The results show that the difference between the radial location of minimum velocity and its corresponding Newtonian value increases when the fluid elasticity increases and that the same is true for the critical angular velocity. The results show that increasing the fluid elasticity increases the velocity gradient near the inner cylinder and so decreases the viscometric viscosity of the fluid (i.e. the fluid behaviour is increasingly shear-thinning) and in consequence $f\mathrm{Re}$. The results also indicate that increasing the radius ratio decreases $f\mathrm{Re}$ in the case of inner cylinder rotation. With increasing radius ratio the velocity profile tends to take a linear form.

References

[1] Escudier, M.P. and Oliveira, P.J. and Pinho, F.T., Fully developed laminar flow of purely viscous non-Newtonian liquids through annuli including the effects of eccentricity and inner cylinder rotation, *Int. J. Heat Fluid Flow*, **23**, 2002, 52-73.

[2] Batra, R.L. and Das, B., Flow of Casson fluid between two rotating cylinder, *Fluid Dyn. Res.*, **9**, 1992, 133-141.

[3] Batra, R.L. and Eissa, M., Helical Flow of a Sutterby model Fluid, *Polym. - Plast. Technol. Eng.*, **33**, 1994, 489-501.

[4] Eissa, M. and Ahmad, S., Forced convection Heat transfer of Robertson- Stiff fluid between two coaxial rotating cylinders, *Int. comm. Heat Mass Transfer,* **26**, 1999, 695-704.

[5] Rao, I.J., Flow of a Johnson-Segalman fluid between rotating co-axial cylinders with and without suction, *Int. J. Non-Linear Mech.*, **34**, 1999, 63-70.

[6] Khellaf, K. and Lauriat, G., Numerical study of heat transfer in a non-Newtonian Carreau- fluid between rotating concentric vertical cylinders, *J. Non- Newtonian Fluid Mech.*, **89**, 2000, 45-61.

[7] Cruz, D.O.A. and Pinho, F.T., Skewed Poiseuille-Couette flow of SPTT fluids in concentric annuli and channels, *J. Non-Newtonian Fluid Mech,* 2004, Article in press.

[8] Phan- Thien, N. and Tanner, R.T., A new constitutive equation derived from network theory, *J. Non- Newtonian Fluid Mech.*, **2**, 1977, 353-365.

[9] Oliveira, P.J. and Pinho, F.T., Analytical solution for fully developed channel and pipe flow of Phan- Thien- Tanner fluids, *J. Fluid Mech.*, **387**, 1999, 271-280.

[10] Alves, M.A. and Pinho, F.T. and Oliveira, P.J., Study of steady pipe and channel flows of single- mode Phan- Thien-Tanner fluid, *J. Non- Newtonian Fluid Mech.*, **101**, 2001, 55-76.

[11] Hashomabadi, S.H. and Etemad, S.Gh. and Thibault, J. and Golkar Naranj, M.R., Analytical solution for dynamic pressurization of viscoelastic fluids, *Int. J. of Heat Fluid Flow,* **24**, 2003, 137-144.

[12] Tanner, R.I., *Engineering Rheology*, Clarendon Press, oxford, 2000.

[13] Mahmud, S. and Fraser, R.A., Analysis of entropy generation inside cylindrical annuli with relative rotation, *Int. J. Thermal Sci.*, **42**, 2003, 513-521.

[14] Gazley, Jr.C. and Monica, C.S., Heat transfer characteristics of the rotational and axial flow between concentric cylinders, in *Trans. of the ASME., paper number 56-A-128, Nov.*25, 1956, 79-90.

[15] Pinho, F.T. and Oliveira, P.J., Axial annular flow of non-linear viscoelastic fluid-an analytical solution, *J. Non- Newtonian Fluid Mech.,* **93**, 2000, 325-337.

[16] Escudier, M.P and Presti, F. Smith, S., Drag reduction in turbulent pipe flow of polymers, *J, Non-Newtonian. Fluid Mech.,* **81**, 1999, 197-213.